11

Analysis of magnetocaloric effect in ferromagnetic shape memory alloy crystals

© G.A. Malygin

Ioffe Institute,
St. Petersburg, Russia

E-mail: malygin.ga@mail.ioffe.ru

Received December 20, 2021
Revised December 20, 2021
Revised December 21, 2021

In the framework of the theory of diffuse martensitic transitions to be based on thermodynamic and kinetic relationships the mechanism of the magnetocaloric (MC) effect in shape memory ferromagnetic alloy crystals is theoretically analysed. The theory adequately describes magnetostructural transformations and MC effect in these crystals at adiabatically applying to them and eliminating from magnetic field. The analysis also includes magneto-anisotropic crystals how to be according to literature data crystals $Ni_{49.5}Mn_{25.4}Ga_{25}$ alloy.

Keywords: magnetocaloric effect, magnetostructural martensite transitions, magneto-anisotropic crystals, isothermal entropy change.

DOI: 10.21883/PSS.2022.05.53518.258

1. Introduction

Shape memory (SM) alloys have a set of functional properties that promote their use as sensing elements and actuators in various micro- and nanoelectronics, robotics, medical and industrial applications. Their sensitivity to mechanical stresses, magnetic and electrical fields facilitate the wide use of these alloys. Recently, researchers have been focused on the investigation of the effect of adiabatic crystal heating and cooling of these alloys near their critical martensitic (phase) transformation temperature. The effect occurs when mechanical stress is quickly applied to or relieved from the crystal [1–6], and for ferromagnets and ferroelectrics — when magnetic field [7–13] or electric field [14] is actuated, respectively. The achieved elastocaloric, magnetocaloric (MC) and electrocaloric effects ΔT_{ad} can be as high as $5-20\,\mathrm{K}$ [1–14]. The adiabatic heating or cooling of the alloy occurs during isothermal change in its entropy in the direct and reverse martensitic transformation processes as first-order phase transitions.

Investigations that have been carried out at present time (reviews [7–9]) show that magnetocaloric effects in ferromagnetic alloys such as NiMnGa(Sn, In) with various nonstoichiometry levels [8,13] are observed in rather narrow temperature ranges ($5-20\,\mathrm{K}$). In addition, they depend on the temperature T and magnetic field strength H at adiabatic variations [8] in a complex and ambiguous way. The specified dependences are influenced by the distance between critical temperatures of martensitic T_c and magnetic T_C transformations [8] and magnetic state of martensite and austenite as well as easy and hard magnetization axes existing in ferromagnetic crystals.

The purpose of the research is to carry out the theoretical study of magnetocaloric effect in Heusler type ferromagnetic alloys subject to transition from cubic phase into tetragonal phase of the lattice. The effect was analyzed and simulated using the smeared thermoelastic martensitic transformations (STMT) theory [15,16], which is based on thermodynamic and kinetic relationships and is sensitive to meso-level crystal structure. It has been successfully used recently for elastocaloric effect analysis of these alloys [5], and before for magnetic shape memory effect analysis of Heusler type ferromagnetic alloys NiMnGa(Sn, In) [17,18]. Section 2 shows the main STMT thermodynamic relations that define isothermal entropy change ΔS of a ferromagnetic crystal and magnetocaloric effect ΔT_{ad} in adiabatic switching on/off of the magnetic field. In Section 3, these relations are used to analyze magnetocaloric effect for magnetic field orientation in the easy magnetization axis direction [001], in Section 4 — if easy and hard magnetization directions exist in the crystal.

2. Magnetocaloric effect and STMT theory

Isothermal entropy change of crystal ΔS that defines the magnetocaloric effect depends on the crystal temperature T and magnetic field H applied to the crystal. This dependence according to the Maxwell's thermodynamic relation [9]:

$$\left(\frac{\partial S}{\partial B}\right)_T = \left(\frac{\partial M}{\partial T}\right)_B \tag{1a}$$

is defined by the integral [8,9,13]:

$$\Delta S(T, B) = \int_0^B \left(\frac{\partial M}{\partial T}\right)_B dB, \tag{1b}$$

where M is the crystal magnetization, $B = \mu_0 H$, μ_0 is the permeability. Taking into account thermodynamically equivalent (1a) relation of S, M, B and T

$$\left(\frac{\partial S}{\partial M}\right)_T = \left(\frac{\partial B}{\partial T}\right)_M, \tag{2a}$$

we obtain an alternative (1b) ratio of isothermal entropy change of crystal ΔS vs. magnetic field B and temperature

$$\Delta S(T, B) = \int_0^M \left(\frac{\partial B}{\partial T}\right)_M dM. \tag{2b}$$

According to the STMT theory, magnetization varies in proportion to the relative volume fraction φ_M of crystal occupied by martensite. Taking into account that austenite can also be a ferromagnet with a relative volume fraction $\varphi_A = 1-\varphi_M$, crystal magnetization is generally described as

$$\begin{aligned} M(T, B) &= m_m \varphi_M(T, B) + m_a\big(1 - \varphi_M(T, B)\big) \\ &= m_a + (m_m - m_a)\varphi_M(T, B), \end{aligned} \tag{3}$$

where m_m and m_a are magnetic moments of martensite and austenite, respectively.

For single-stage martensitic transformation, the volume fraction of martensite is defined by thermodynamic relation [{]15,16}:

$$\varphi_M = \frac{1}{1 + \exp(\Delta U / k_B T)}, \tag{4a}$$

where $\Delta U = \omega \Delta u$ is the change in free energy of the alloy when a martensitic phase nucleus with a volume of ω is formed, Δu is the bulk density of the phase transition free energy,

$$\Delta u = q_0 \frac{T - T_{c0}}{T_{c0}} - \Delta m_M B, \tag{4b}$$

Herein, $q_0 = \Delta S_c T_{c0}$ is the transition heat, T_{c0} is the martensitic transformation temperature without magnetic field, ΔS_c is the entropy change in martensitic transformation, k_B is the Boltzmann's constant, $\Delta m_{MA} B$ is the bulk density of martensite magnetic energy due to the martensite austenite magnetization difference $\Delta m_{MA} = \Delta m_{ma} V_0$, where $\Delta m_{ma} = m_m - m_a$ is their magnetic moment difference, V_0 is the atomic volume of the alloy. For the following analysis, it is convenient to write exponential equation (3a) in dimensionless variables

$$\varphi_M(\overline{T}, \overline{B}) = \frac{1}{1 + \exp[\overline{\omega}(\overline{T} - 1 - \overline{B})]}, \tag{5a}$$

where $\overline{T} = T/T_{c0}$, $\overline{B} = B/B_M$, $B_M = q_0/\Delta m_{MA}$, $\overline{\omega} = q_0\omega/k_B T \approx q_0\omega/k_B T_{c0}$. When solving (5a) for field B, we obtain the field dependence on the martensite temperature and concentration:

$$B = B_M\left(\frac{T}{T_{c0}} - 1 + \frac{1}{\overline{\omega}} \ln\left(\frac{\varphi_M}{1 - \varphi_M}\right)\right). \tag{5b}$$

Partial temperature derivative for B is equal to Clausius–Clapeyron coefficient,

$$\left(\frac{\partial B}{\partial T}\right)_{\varphi_M} = \frac{B_M}{T_{c0}} = \frac{q_0}{\Delta m_{MA} T_{c0}}. \tag{5c}$$

As a result, for isothermal entropy change of crystal, we obtain the following according to (2b)

$$\begin{aligned} \Delta S_M(T, B) &= \frac{q_0}{\Delta m_{MA} T_{c0}} \Delta M, \\ \Delta M(T, B) &= M(T, B) - M(T, 0). \end{aligned} \tag{6}$$

Then, taking into account the relation between the magnetocaloric effect ΔT_{ad}^M and isothermal entropy change ΔS_M,

$$\Delta T_{ad}^M = \Delta S_M T_{c0} / C_p, \tag{7a}$$

we obtain the final relation

$$\begin{aligned} \Delta T_{ad}^M(\overline{T}, \overline{B}) &= \frac{q_0}{C_p} \Delta\varphi_M(\overline{T}, \overline{B}), \\ \Delta\varphi_M(\overline{T}, \overline{B}) &= \varphi_M(\overline{T}, \overline{B}) - \varphi_M(\overline{T}, 0), \end{aligned} \tag{7b}$$

where $C_p = V_0 C_p$ is the specific heat of the alloy. According to equation (7b), magnetocaloric effect depends on the martensitic transformation temperature q_0 and the amount of martensite $\Delta\varphi_M(T, B)$induced by the magnetic field. Isothermal entropy equation (1b) taking into account isothermal entropy dependence not only on the amount of martensite, but also on the crystal magnetization will be used in Section 4 to discuss the crystal magnetic anisotropy under magnetocaloric effect.

3. Magnetocaloric effect in the absence of magnetic anisotropy

$Ni_{50+x+y}Mn_{25-x}(Ga,Sn,In)_{25-y}$ alloys with various degree of deviation from the stoichiometric ratio ($x + y = 0–6\%$) have various complex influence on the magnetic properties of the alloy and magnetocaloric effect parameters [8,12,13]. High-temperature phase of the stoichiometric ratio of Ni_2MnGa has a BCC lattice that transforms into tetragonal martensite at temperatures below 200 K which is accompanied with crystal compression strain $\varepsilon_m = 6\%$ in axis [001] direction. Alloy state deviation from the stoichiometric ratio is accompanied with the martensitic transformation temperature growth T_c above room temperature [19,20]until the temperature T_c achieves $T_C = 340–370$ K for ferromagnetic state transition of the given alloys into paramagnetic state. Alloy crystals are anisotropic in the magnetic field application direction. Field application along cubic axes (010) and (100) requires a higher field strength compared with direction [001] to achieve the crystal magnetization saturation.

Magnetocaloric effect analysis is carried out herein in conditions no complicated by magnetic and anisotropic effects and magnetic moment dependence of martensite m_m

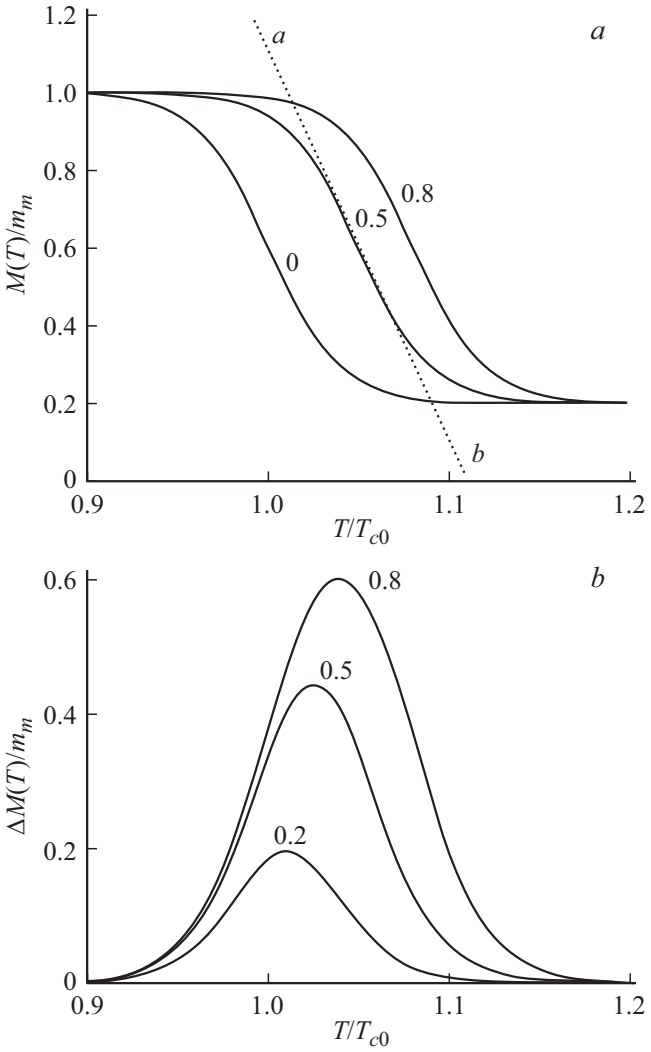

Figure 1. Temperature dependences of magnetization $\overline{M} = M/m_m$ (a) and magnetization difference $\Delta\overline{M} = \Delta M/m_m$ (b) of the alloy crystal according to equations (3) and (6) at three induction values $\overline{B} = B/B_M$ (numerals near the curves) and $\overline{\omega} = 50$.

and austenite m_a on the magnetic field strength. In Fig. 1, a, the curves demonstrate the crystal magnetization dependence on temperature in dimensionless coordinates according to equation (3) near the martensitic transformation temperature $\overline{T} = 0.9{-}1.2$ at three reduced induction values $\overline{B} = 0$, 0.5, 0.8 and dimensionless martensite nucleus volume $\overline{\omega} = 50$,

$$\overline{M}(\overline{T}, \overline{B}) = \overline{m}_a + (1 - \overline{m}_a)\varphi_M(\overline{T}, \overline{B}), \qquad (8a)$$

where $\overline{M} = M/m_m$, $\overline{m}_a = m_a/m_m = 0.2$. In Fig. 1, a, a dotted line abshows the slope of curves $M(\overline{T})$ at $\overline{T}_c = T_c/T_{c0}$,

$$\left(\frac{\partial\overline{M}}{\partial\overline{T}}\right)_{\overline{T}_c} = -\overline{\omega}(1 - \overline{m}_a)\varphi_c(1 - \varphi_c),$$

$$\varphi_c = \frac{1}{2}(\varphi_m + \varphi_a), \qquad (8b)$$

where $\varphi_m = M_m^m/m_m$, $\varphi_a = M_a^a/m_a$, M_m^m and M_a^a are magnetization limits of martensite and austenite. Martensitic transformation temperature interval (temperature smearing) $\Delta\overline{T}$ is defines as follows

$$|\Delta\overline{T}| \approx (\overline{M}_m - \overline{M}_a)/(\partial\overline{M}/\partial\overline{T})_{\overline{T}_c} = \frac{\varphi_m - \varphi_a}{\overline{\omega}\varphi_c(1 - \varphi_c)}. \qquad (9)$$

According to (9), the transformation temperature interval is increased with the decrease in the phase transformation $\Delta T \sim 1/\overline{\omega}$. With $\varphi_a = 0$ and $\varphi_m = 1$, the temperature interval is maximum and equal to $(4/\overline{\omega})T_{c0}$.

Magnetocaloric effect $\Delta T_{ad}^M \sim \Delta S_M$ and isothermal entropy change ΔS_M in adiabatic jump of magnetic field B depend on the difference of crystal magnetization in magnetic field and without magnetic field $\Delta M(T, B)$ according to equations (6) and (7) . This difference is mainly defined by the change in the martensite bulk concentration in the crystal $\Delta\varphi_M(T, B)$ (7). Fig. 1, b shows the magnetization difference dependence $\Delta\overline{M} = \Delta M/m_m$ on temperature $\overline{T} = T/T_{c0}$ according to induction $\overline{B}$ and transformation volume $\overline{\omega}$ indicated in Fig. 1, a. Magnetization difference is increased with the magnetic field strength and transformation volume growth and achieves its maximum value $\Delta M_{\max}(T_{\max}, B)$ at $\overline{T}_{\max} = 1 + \overline{B}$. Dependence $\Delta\overline{M}_{\max}(B)$ at three values $\overline{\omega} = 50$, 75 and 150 is shown in Fig. 2. The calculation shows that with induction growth, magnetocaloric effect $\Delta T_{ad}^M \sim \Delta S^M \sim \Delta M_{\max}(B, \omega)$ achieves saturation the faster, the higher transformation volume ω is, i.e. the smaller martensitic transformation temperature range $\Delta T \sim 1/\omega$ is. It also can be seen that magnetocaloric effect, as opposed to elastocaloric

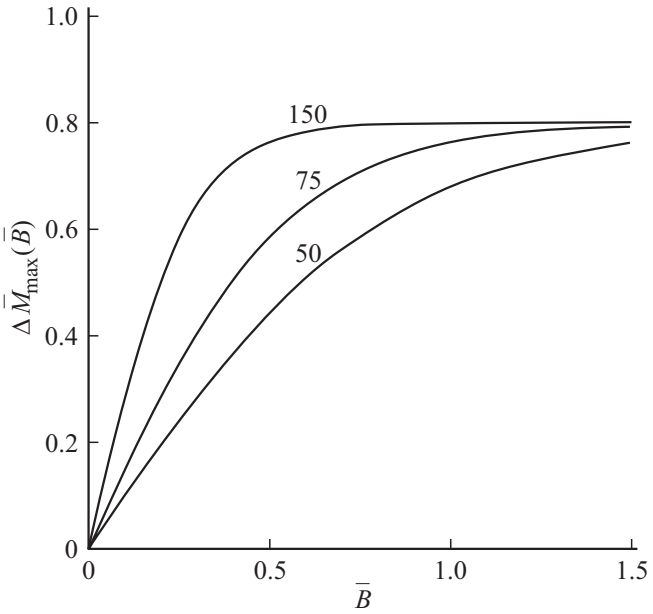

Figure 2. Dependence of the maximum crystal magnetization variation $\Delta\overline{M}_{\max}(\overline{B})$ on magnetic field $\overline{B} = B/B_M$ at three dimensionless transformation volume values $\overline{\omega} = 50$, 75 and 150 (numerals near the curves).

effect, is observed in rather narrow temperature interval $\approx 0.1T_{c0} = 20-30$ K at $T_{c0} = 200-300$ K.

4. Magnetic anisotropy influence on the magnetocaloric effect

Experiments [8,13] show that, with magnetic field orientation along the easy magnetization direction [001], deviation from the stoichiometric ratio of Ni–Mn–Ga as a result of Ni atom concentration growth and respective loss of Mn atoms is accompanied with the critical martensitic transformation temperature growth T_c. In addition, the ratio of martensite and austenite magnetization is changed. When Ni concentration is lower than 51.5%, martensite magnetization is lower than austenite magnetization. But in both cases, in changes nonlinearly with the magnetic field strength growth [8,13] and depends on the magnetic field orientation with reference to the easy crystal magnetization direction. martensite twinning with formation of five- and seven-layered structural domains with boundaries which simultaneously serve as magnetic domain boundaries is a source of magnetic stresses $\sigma_M(B)$ and magnetic anisotropy energy $W_a(B) = \varepsilon_{tw}\sigma_M(B)$ [18,22], where ε_{tw} is the twinning strain in lattice restructuring. As a result, for SM alloy crystal magnetization, we have the following

$$M(T,B) = m_m(B)\varphi_M(T,B) + m_a(B)\big(1-\varphi_M(T,B)\big) = m_a(B) + \big(m_m(B) - m_a(B)\big)\varphi_M(T,B). \quad (10a)$$

Martensite concentration in equation (10a) generally can depend on the magnetic anisotropy energy W_a (Appendix A):

$$\varphi_M(T,B) = \frac{1}{1+\exp\left[\overline{\omega}\Big((T-T_{c0})/T_{c0} - 1 - \big(\Delta m(B)B + W_a(B)\big)/q_0\Big)\right]}, \quad (10b)$$

and magnetic moments of martensite m_m and austenite m_a depend on the magnetic field [23]. And the magnetic moment of martensite also depends on the magnetic field orientation with respect to the easy magnetization direction [001],

$$m_m(B,\beta) = m^{\infty}_{[001]}\,\mathrm{th}\,(B/B_{[001]})\cos\beta^2 + m^{\infty}_{[100]}\,\mathrm{th}\,(B/B_{[100]})\sin\beta^2, \quad (11)$$

$$m_a(B) = m^{\infty}_a\,\mathrm{th}\,(B/B_a).$$

Here β is the angle between the crystal axis [001] and magnetic field direction, m^{∞}_m and m^{∞}_a are magnetic moments in crystal saturation with magnetic field. $B_{[100]} = k_B T/m^{\infty}_{[100]}$, $B_{[001]} = k_B T/m^{\infty}_{[001]}$, $B_a = k_B T/m^{\infty}_a$ [23].

Fig. 3, *a* shows the calculations of magnetic moments of martensite in easy magnetization direction ([001], $\beta = 0$) and hard magnetization direction ([100], $\beta = \pi/2$) according to equations (11). Fig. 3, *b* shows the difference

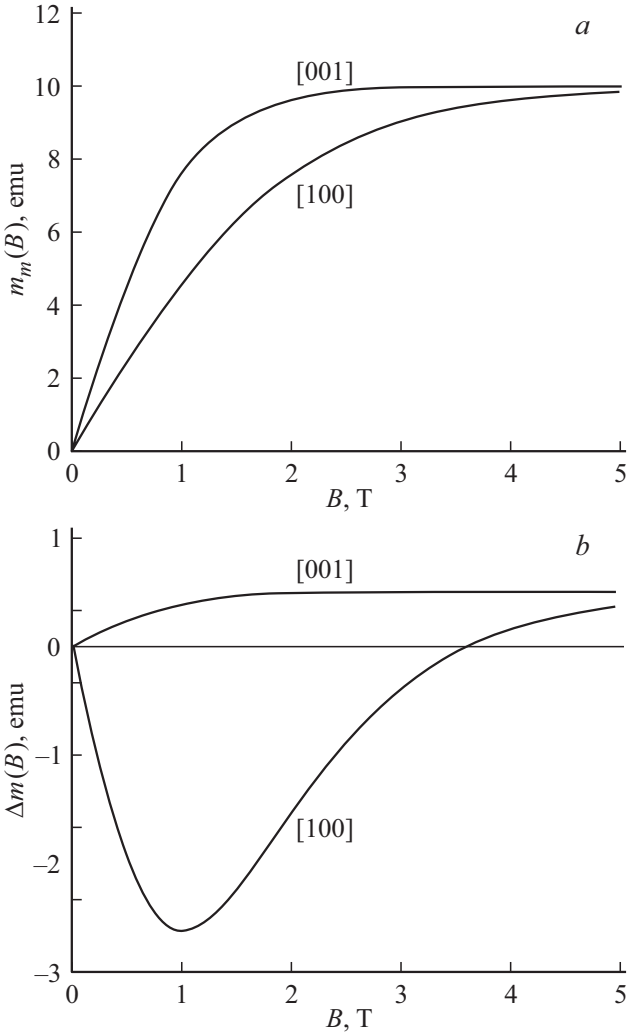

Figure 3. Magnetic field dependence B of the martensite magnetic moments (a) and difference Δm of magnetic moments of martensite and austenite (b) with field orientation along the easy magnetization direction [001] and hard magnetization direction [100], respectively.

$\Delta m(B)$ of magnetic moments of martensite $m_m(B)$ and austenite $m_a(B)$. It can be seen that the shown difference depends significantly on the magnetic field orientation with respect to the easy magnetization direction. The results shown in Fig. 3 have been obtained at following parameters: $m^{\infty}_{[001]} = m^{\infty}_{[100]} = 10$, $m^{\infty}_a = 9.5\,\mathrm{A}\cdot\mathrm{m}^2$, $B_{[001]} = 1$, $B_{[100]} = 2$ and $B_a = 1$ T (Tesla). It shall be noted that the magnetic moment difference of martensite and austenite $\Delta m(B) = m_m(B) - m_a(B)$ ambiguously depends on the magnetic field strength with orientation along the hard magnetization direction.

Temperature dependences of crystal magnetization shown in Fig. 4 also demonstrate significant difference between the field directions along axes [001] and [100] according to equations (10). In the first case (Fig. 4, *a*), martensite magnetization is a little higher than austenite magnetization,

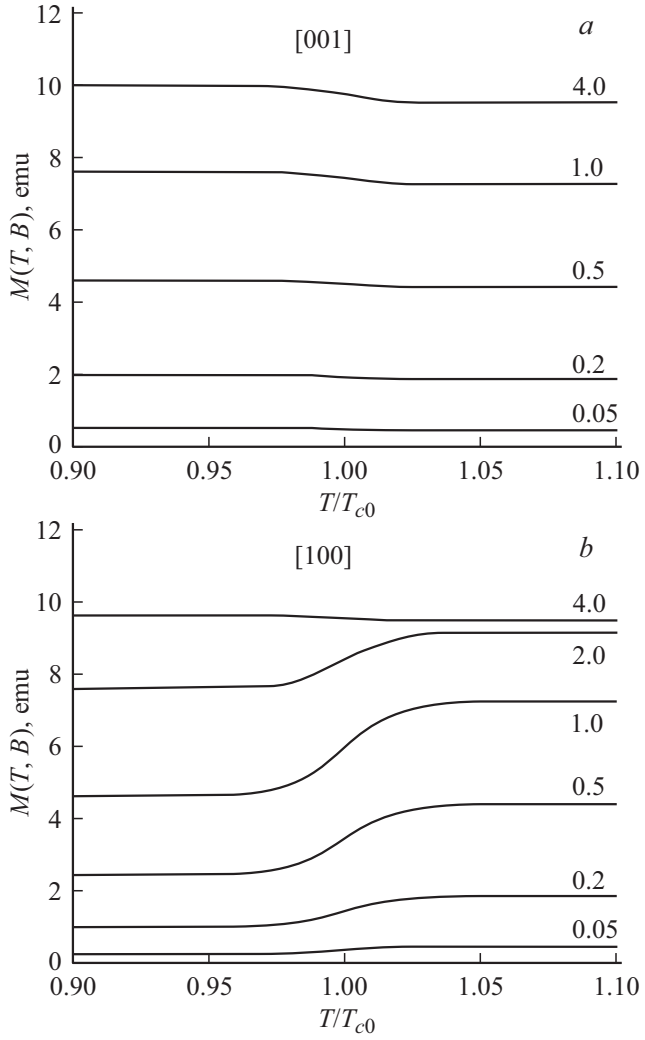

Figure 4. Temperature dependences of crystal magnetization with magnetic field orientation along the easy magnetization direction [001] (a) and hard magnetization direction [100] (b), respectively. Numerical values near the curves are magnetic field strength B in T.

in the second case (Fig. 4, b), it is considerably higher with austenite. Such form of temperature dependences of magnetization is typical of $Ni_{49.5}Mn_{25.4}Ga_{25}$ [8,13] crystals with composition close to stoichiometric ratio. It is also distinguished by low dependence of the critical martensitic transformation temperature T_c on the magnetic field at least at moderate fields. This has been considered in the curves in Fig. 4 and means that the main change in the crystal magnetization with the magnetic field strength growth is associated with magnetic moment growth, rather than with the change in the martensite volume fraction (Section 3).

Adiabatic switching on/off of the the magnetic field causes the change in the structural state of the alloy (austenite-to-martensite transformation and reverse transformation) and is accompanied with the change in the crystal magnetization (equation (10a)):

$$\Delta M(T,B) = \big(m_m(B) - m_a(B)\big)\varphi_M(T,B). \qquad (12)$$

According to the thermodynamic relation (1b), isothermal entropy change of crystal is equal to:

$$\Delta S(T,B,\beta) = \int_0^B \left(\frac{\partial \Delta M}{\partial T}\right)_B dB$$

$$= \left(\frac{\partial \varphi_M}{\partial T}\right)_B \int_0^B \big(m_m(B,\beta) - m_a(B)\big)dB, \qquad (13a)$$

where [15,16]

$$\left(\frac{\partial \varphi_M}{\partial T}\right)_B = -\overline{\omega} T_c^{-1}\, \varphi_M(1-\varphi_M). \qquad (13b)$$

As a result, we obtain the following relation for crystal entropy change in magnetostructural transition

$$\Delta S(T,B,\beta) = -\overline{\omega} T_c^{-1}\, \varphi_M(T)\big(1-\varphi_M(T)\big)\Delta M_m^a(B,\beta). \qquad (13c)$$

Derivative $(\partial\varphi_M/\partial T)_B$ is outside the integral sign (13a), since the experiment [8,13] suggests that magnetic field has no essential influence on the martensite concentration, but has essential influence on the crystal magnetization kinetics $\Delta M_m^a(B,\beta)$ (Appendix B). According to equation (13b), the temperature derivative achieves its maximum value $\overline{\omega}/4T_{c0}$ at martensite volume fraction $\varphi_M = 1/2$, i.e. at critical transformation temperature $T = T_{c0}$. Fig. 5 shows the calculation results according to equations (13) of dependence of isothermal entropy change ΔS on field B at temperature

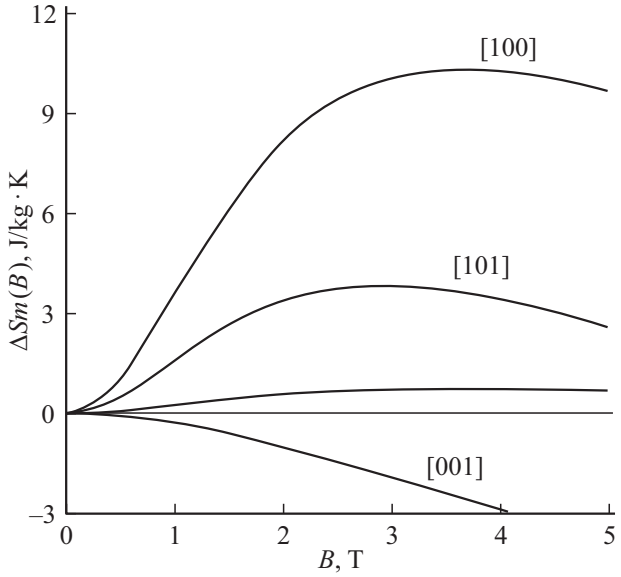

Figure 5. Dependence of isothermal entropy ΔS on magnetic field B with adiabatic switching on and with the magnetic field directions in the alloy crystal shown in the Figure.

$T = T_{c0} = 200\,\mathrm{K}$, $\overline{\omega} = 100$ and martensite and austenite magnetization values shown above (Fig. 3 and 4). Curves in Fig. 5 show dependences $\Delta S(B)$ for three magnetic field orientations with respect to crystal axes. It can be seen that with field orientation in easy magnetization direction [001], entropy is negative and is low compared with its positive values with magnetic field orientation along more hard magnetization directions. Its positive value shown in Fig. 5 means that adiabatic switching on of the magnetic field is accompanied with the crystal heating. It is obvious that during the adiabatic switching off of the magnetic field, an opposite refrigerating magnetocaloric effect will be observed, $\Delta S < 0$, i.e. crystal temperature reduction, $\Delta T_{ad} < 0$. According to equation (7a), magnetocaloric effect ΔT_{ad} is directly proportional to the entropy change ΔS of the crystal undergoing martensitic transformation. In case addressed herein, it is described with the following equation

$$\Delta T_{ad}(T, B, \beta) = \frac{T_{c0}}{C_p}\Delta S(T, B, \beta) = -\frac{\overline{\omega}}{C_p}\varphi_M(T)\big(1 - \varphi_M(T)\big)\Delta M_m^a(B, \beta). \quad (14)$$

Fig. 6 shows the magnetocaloric effect dependence on the temperature T at $T_{c0} = 200\,\mathrm{K}$, $C_p = 400\,\mathrm{J/kg \cdot K}$ and several magnetic induction values B, when magnetic induction growth increases the crystal temperature reduction. Equation (14) also shows that MC effect is increased with the phase transformation volume growth as follows

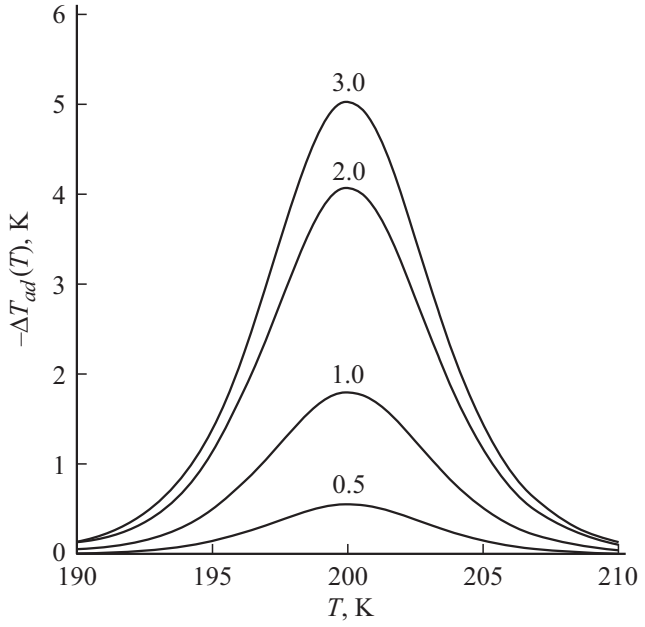

Figure 6. Temperature dependences of magnetocaloric effect ΔT_{ad} with magnetic field orientation along the hard magnetization direction [100] and adiabatic magnetization switching off from the magnetic field strengths B shown in the Figure (numeric values shown at the curves in T).

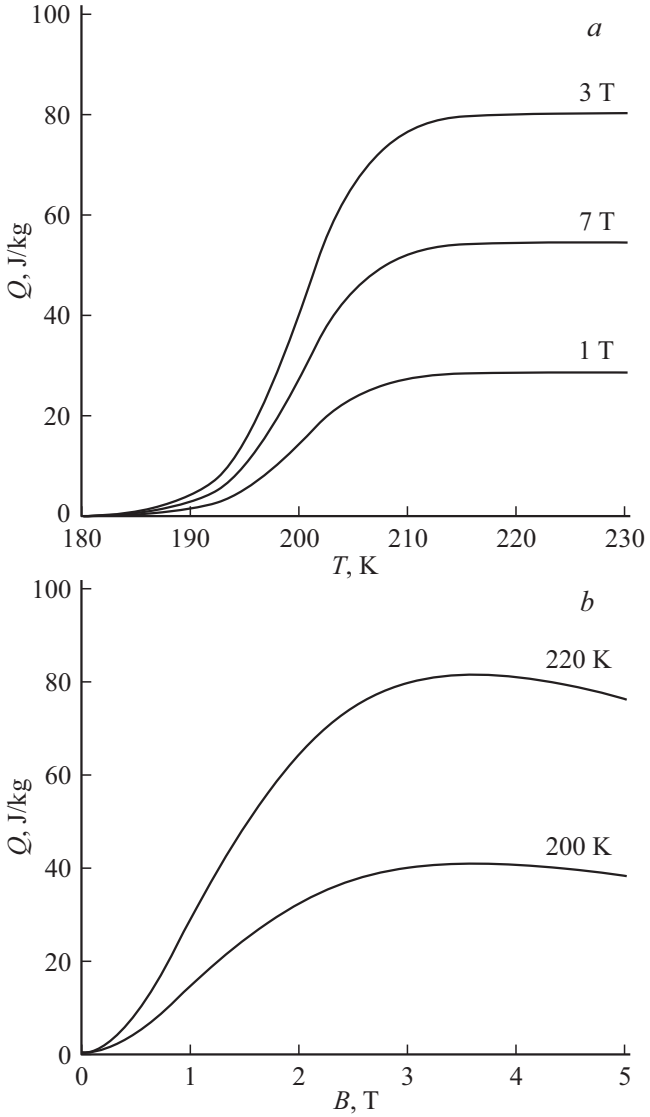

Figure 7. Temperature (a) and field (b) dependences of cold capacity of the alloy Q with adiabatic switching off of magnetic field from the magnetic field strengths B and temperatures T, respectively, shown in the figures (numeric values near the curves).

$\Delta T_{ad} \sim \overline{\omega} \sim \omega$, i.e. with martensitic transformation temperature range reduction $\Delta T \sim 1/\omega$. Results of theoretical analysis of magnetocaloric effect according to STMT theory shown in Fig. 4–6 match well with the results of the experimental investigation in $Ni_{49.5}Mn_{25.4}Ga_{25}$ [8,13] crystals.

In conclusion, we will find an important characteristic of magnetocaloric effect and solid-state refrigerating devices using MC effect according to the STMT theory. This amount of heat Q that can be absorbed by a device, i.e. its cold capacity,

$$Q(T, B, \beta) = \int_0^T \Delta S(T, B, \beta)dT. \quad (15a)$$

According to the calculation results shown in Fig. 5, isothermal entropy change has its maximum negative value with magnetic field orientation along the hard magnetization direction [100]. Using the magnetization component in equation (13c) and Appendix B as a limiting value:

$$\Delta M_m^a(T, B, \pi/2) = m_{[100]}^{\infty} B_{[100]} \ln\left(\mathrm{ch}\left(\frac{B}{B_{[100]}}\right)\right) - m_a^{\infty} B_a \ln\left(\mathrm{ch}\left(\frac{B}{B_a}\right)\right), \quad (15b)$$

we obtain, after numerical solution of equation (15a), dependence of the heat Q on the temperature at three magnetic field strengths B (Fig. 7, *a*). Fig. 7, *b* shows dependence of the cold capacity Q on the magnetic field at two temperatures (numeric values near the curves). It can be seen that at $B \approx 3.5\,\mathrm{T}$ and $T > 220\,\mathrm{K}$, alloy cold capacity per unit of weight achieves its maximum $\approx 80\,\mathrm{J/kg}$ (atomic weight of the given (simulated) Ni−Mn−Ga alloy is 60.5 g). This value is approximately twice as high as that of Gd crystal 43.8 J/kg [24].

5. Conclusion

Within the theory of first-order phase transitions based on thermodynamic and kinetic relations, including structural martensitic transformations in shape memory alloys, theoretical analysis was carried out to investigate the influence of magnetic field on the structural transition kinetics in Heusler type ferromagnetic alloy crystals and the magnetocaloric effect associated with this influence. The analysis has shown that the smeared thermoelastic martensitic transformation theory adequately describes the dependences of magnetocaloric effect on the temperature and magnetic field at adiabatic variations of the magnetic field observed during the experiment with $Ni_{49.5}Mn_{25.4}Ga_{25}$ [8,13] crystals.

Annex A

By introducing designations $f = \cos\beta^2$ and $1-f = \sin\beta^2$ and using equation (10c) from the main text and magnetic strain relation [22]

$$\sigma_{\mathrm{magn}}(B) = \varepsilon_{tw}^{-1} \frac{\partial}{\partial f} \int_0^B m_m(B, f) dB, \quad (1A)$$

we obtain that the magnetic anisotropy energy $W_a = \varepsilon_{tw}\sigma_{\mathrm{magn}}$ is described as follows

$$W_a(B) = m_{[001]}^{\infty} B_{[001]} \ln\left(\mathrm{ch}\left(\frac{B}{B_{[001]}}\right)\right) - m_{[100]}^{\infty} B_{[100]} \ln\left(\mathrm{ch}\left(\frac{B}{B_{[100]}}\right)\right), \quad (2A)$$

With $B \to \infty$, it linearly depends on the magnetic field,

$$W_a(B \to \infty) = (m_{[001]}^{\infty} - m_{[100]}^{\infty})B + (m_{[100]}^{\infty} B_{[100]} - m_{[001]}^{\infty} B_{[001]}) \ln 2, \quad (3A)$$

and with $m_{[001]}^{\infty} = m_{[100]}^{\infty} = m_s$ tends to the limit [18]

$$W_a^{\infty} = m_s(B_{[100]} - B_{[001]}) \ln 2.$$

Annex B

By substituting relations (10c) and (10d) in integral (13a) in the main text, we obtain

$$\Delta M_m^a(B, \beta) = \int_0^B \big(m_m(B, \beta) - m_a(B)\big) dB$$
$$= m_{[001]}^{\infty} B_{[001]} \ln\left(\mathrm{ch}\left(\frac{B}{B_{[001]}}\right)\right)(\cos\beta)^2 + m_{[100]}^{\infty} B_{[100]} \ln\left(\mathrm{ch}\left(\frac{B}{B_{[100]}}\right)\right)(\sin\beta)^2 - m_a^{\infty} B_a \ln\left(\mathrm{ch}\left(\frac{B}{B_a}\right)\right).$$

Conflict of interest

The author declares that he has no conflict of interest.

References

[1] E. Bonnot, R. Romero, L. Mañosa, E. Vives, A. Planes. Phys. Rev. Lett. **100**, 125901 (2008).
[2] L. Mañosa, S. Jarque-Farnos, E. Vives, A. Planes. Appl. Phys. Lett. **103**, 211904 (2013).
[3] F. Xiao, M. Jin, J. Liu, X. Jin. Acta Mater. **96**, 292 (2015).
[4] D. Zhao, F. Xiao, Zh. Nie, D. Cong, W. Sun, J. Liu. Scripta Mater. **149**, 6 (2018).
[5] G.A. Malygin, FTT, **64**, 255 (2022) (in Russian).
[6] X-M. Huang, L-D. Wang, H-X. Liu, H-L. Yan, N. Jia, B. Yang, Z-B. Li, Yu-D. Zhang, C. Esling, X. Zhao, L. Zuo. Intermetallics **113**, 106579 (2019).
[7] K.A. Gschneidner, V.K. Pecharsky, A.O. Tsokol. Rep. Prog. Phys. **68**, 1479 (2005).
[8] A. Planes, L. Mañosa, M. Aset. J. Phys.: Condens. Matter **21**, 233201 (2009).
[9] T. Brück, J. Phys. D **38**, R381 (2005).
[10] L. Mañosa, S. Jarque-Farnos, E. Vives, A. Planes. Appl. Phys. Lett. **103**, 211904 (2013).
[11] F. Xiao, M. Jin, J. Liu, X. Jin. Acta Mater. **96**, 292 (2015).
[12] F. Hu, B. Shen, J. Sun, G. Wu. Phys. Rev. B **64**, 132412 (2001).
[13] J. Marcos, A. Planes, L. Mañosa, F. Casanova, X. Battle, A. Labarta, B. Martinez. Phys. Rev. B **66**, 224413 (2002).
[14] A.S. Mishenko, Q. Zhang, J.F. Scott, R.W. Wathmore, N.D. Mathur. Science **311**, issue 5765, 1270 (2006).
[15] G.A. Malygin, Physics of the Solid State **36**, 1489 (1994) (in Russian)..

[16] G.A. Malygin, UFN, **171** 187 (2001) (in Russian).
[17] G.A. Malygin, ZhTF **77**, *8*, 136 (2007) (in Russian).
[18] G.A. Malygin, FTT, **51**, 1599 (2009) (in Russian).
[19] A.N. Vasiliev, V.D. Buchel'nikov, T. Takagi, V.V. Khovailo, E.I. Estrin. UFN, **173**, (577) (2003) (in Russian).
[20] M. Richard, J. Feuchtwanger, D. Schlagel, T. Lograsso, S.M. Allen, R.C. O'Handley. Scripta Mater. **54**, 1797 (2006).
[21] G.A. Malygin, FTT, **63**, 272 (2021) (in Russian).
[22] A.A. Lichachev, A. Sozinov, K. Ullakko. Mater. Sci. Eng. A **378**, 513 (2004).
[23] J. Smart. Effektivnoie pole v teorii magnetizma. Mir, M. (1968). 271 s. (in Russian).
[24] V.I. Mityuk, N.Yu. Pankratov, G.A. Govor, S.A. Nikitin, A.I. Smarzhevskaya. FTT **54**, 1865 (2012) (in Russian).